

1 **A high-efficiency scar-free genome editing toolkit for *Acinetobacter***
2 ***baumannii***

3

4 Rubén de Dios¹, Kavita Gadar¹ and Ronan R McCarthy¹

5 ¹Division of Biosciences, Department of Life Sciences, Centre of Inflammation Research and
6 Translational Medicine, College of Health and Life Sciences, Brunel University London,
7 Uxbridge, UB8 3PH, UK.

8

9

10

11

12

13

14

15

16

17

18

19

20

21

22 Running title: Scar-free mutagenesis in *Acinetobacter baumannii*

23 Corresponding author: Ronan R McCarthy ronan.mccarthy@brunel.ac.uk

24

25 **Structured synopsis**

26 Background: The current mutagenesis tools for *Acinetobacter baumannii* leave selection
27 markers or residual sequences behind, or involve tedious counterselection and screening
28 steps. Furthermore, they are usually adapted for model strains, rather than to multidrug
29 resistant (MDR) clinical isolates.

30

31 Objectives: To develop a scar-free genome editing tool suitable for chromosomal and plasmid
32 modifications in MDR *A. baumannii* AB5075.

33

34 Methods: We prove the efficiency of our adapted genome editing system by deleting the
35 multidrug efflux pumps *craA* and *cmlA5*, as well as curing plasmid p1AB5075. We then
36 characterised the antibiotic sensitivity phenotype of the mutants compared to the wild type
37 for chloramphenicol, tobramycin and amikacin by disc diffusion assays and determined their
38 minimum inhibitory concentration for each strain.

39

40 Results: We successfully adapted the genome editing protocol to *A. baumannii* AB5075,
41 achieving a double recombination frequency close to 100% and securing the construction of a
42 mutant within 10 work days. Furthermore, we show that the Δ *craA* has a strong sensitivity to
43 chloramphenicol, tobramycin and amikacin, whereas the Δ *cmlA5* mutant does not show a
44 significant decrease in viability for the antibiotics tested. On the other hand, the removal of
45 p1AB5075 produced an increased sensitivity to tobramycin and amikacin.

46

47 Conclusion: We have adapted a highly efficient genome editing tool for *A. baumannii* and
48 proved that *craA* has a broader substrate range than previously thought. On the other hand,
49 whereas *cmlA5* is annotated as a chloramphenicol efflux pump and is encoded within an
50 aminoglycoside resistance island, it does not provide resistance to any of those compounds.

51

52

53

54

55 **Introduction**

56 *A. baumannii* is an aerobic Gram-negative bacterium that is widespread in the environment
57 and inhabits different niches. However, it can also be an opportunistic pathogen that infects
58 immunocompromised patients.^{1,2} Nowadays, it is estimated that up to 10% of nosocomial
59 infections in the United States and 2% in Europe are caused by this pathogen, with these
60 frequencies almost doubling in Asia and the Middle East. Furthermore, around 45% of *A.*
61 *baumannii* isolates in global terms exhibit multi-drug resistance (MDR, i.e. resistance to at
62 least 3 classes of antibiotics), with local rates rocketing to 70% in Latin America and the
63 Middle East.^{1,3-5} Due to this, *A. baumannii* has been included among the most concerning
64 MDR pathogens under the acronym *ESKAPE* (*Enterococcus faecium*, *Staphylococcus aureus*,
65 *Klebsiella pneumoniae*, *A. baumannii*, *Pseudomonas aeruginosa* and *Enterobacter spp.*).⁶
66 Moreover, a World Health Organisation (WHO) report highlighted carbapenem-resistant *A.*
67 *baumannii* as a priority pathogen, for which novel therapeutic approaches urgently need to be
68 developed.⁷

69 The recalcitrance of this species to treatment is due to its capacity for resistance and
70 persistence,¹ aided by its multiple MDR mechanisms. These include the cell envelope as a
71 barrier, multi-drug efflux systems and mutations in genes coding for porins and antibiotic
72 targets (e.g. ribosomal proteins, penicillin binding proteins, DNA replication enzymes and the
73 lipid A biosynthetic pathway), as well as enzymes that degrade/inactivate antibiotics.²
74 Oftentimes, these features can spread among the population through mobile genetic elements
75 and the ability of *A. baumannii* to be naturally competent.^{2,8-10}

76 With technological advances, genome editing tools have evolved, allowing precise genome
77 editing (i.e. insertions and deletions), from a single nucleotide to dozens of kilobases.
78 However, this progress is often uneven, with tools being biasedly developed for a few well
79 established model organisms. In the case of *A. baumannii*, many simple targeted genetic tools
80 have been adapted for their use in model strains of this pathogen. These tools go from gene
81 disruption by plasmid insertion in a single recombination event to mutation by antibiotic
82 resistance marker insertion.¹¹ Next-step strategies include recombineering-based gene
83 disruption followed by removal of the selection marker by site-specific recombination,
84 allowing the use of the same marker for subsequent rounds of mutation to construct multiple
85 mutants.¹² Even more refined, some protocols allow scar-less gene modification by double
86 recombination aided by a counterselectable marker.¹³ Moreover, after the bloom of clustered
87 regularly interspaced short palindromic repeats (CRISPR)-Cas systems as a molecular

88 biology tool, a CRISPR interference (CRISPRi) kit has been developed for *A. baumannii* that
89 allows knocking down the expression of both essential and non-essential genes.¹⁴
90 However, depending on the purpose they are intended for, these genetic editing methods can
91 have some limitations. Gene disruption is not always desirable due to the limited amount of
92 selection markers available and possible polar effects within operons. Strategies including
93 marker removal are usually based on site-specific recombinases that leave a scar in the
94 genome.^{12,15} However this recombinogenic sequence may cause genomic instability after
95 successive rounds of mutation.¹⁶ These drawbacks can be prevented by counterselection-
96 mediated scar-free strategies, which allow more complex genome manipulation (i.e. targeted
97 point mutations, domain truncations, allele exchange, deletion of whole clusters), but
98 counterselection often requires passaging under pressing selection and tedious screening for
99 clones that underwent a second recombination event. Furthermore, the current tools are
100 mainly developed for model *A. baumannii* strains, which can be less representative as
101 compared to the prevalent clinical isolates. Besides, an extra limitation appears when
102 applying these tools to MDR *A. baumannii* strains due to the little availability of selection
103 markers.

104 In our efforts to implement state-of-the-art methodologies for standardisation of genome
105 editing in non-model MDR *A. baumannii* strains, we have adapted an accelerated highly
106 efficient SceI-based mutagenesis method,¹⁷⁻²⁰ developed and optimised for *Pseudomonas*
107 *putida*,^{16,21} to MDR *A. baumannii* AB5075.³ For this, we have modified the two plasmids
108 used in this system with selectable markers that can be used in this strain and subsequently
109 adapted the protocol pipeline. As a proof of concept, we have constructed an in-frame
110 deletion mutant in *craA*, a gene encoding a dedicated chloramphenicol-specific efflux pump.
111 Afterwards, we have attempted to address the function of *cmlA5*, a putative plasmid-borne
112 chloramphenicol efflux pump coding gene inferred from homology, by comparison with the
113 *craA* mutant. As a result, we have validated the utility of this system for scar-free
114 chromosomal and plasmid editing in *A. baumannii* AB5075.

115

116 **Materials and Methods**

117 Bacterial strains and culture media

118 *A. baumannii* AB5075 (VIR-O colony morphotype),^{3,22,23} its derivative mutants and *E. coli* host
119 strains (DH5 α and DH5 α λ *pir*) were routinely grown in liquid or solid LB (Miller) at 37 °C
120 (180 rpm or static, respectively).^{16,24} When necessary, LB was supplemented with kanamycin
121 (25 mg/L), ampicillin (100 mg/L), apramycin (60 mg/L for *E. coli*, 200 mg/L for *A.*

122 *baumannii*), tetracycline (5 mg/L) or tellurite (6 mg/L for *E. coli*, 30 mg/L for *A. baumannii*).

123 A summary of strains used in this work is shown in Supplementary Table S1.

124

125 Plasmid construction

126 A list of plasmids and primer sequences used in this work can be found in Supplementary
127 Table S1. All plasmid derivatives were constructed using standard restriction-based
128 molecular cloning.

129 pEMG-Tel (pEMGT) was constructed by cloning a DNA fragment from pMo130-TelR
130 (Addgene, #50799) (bearing the Tel resistance marker) digested with SmaI in pEMG cut with
131 AflIII and blunted with Klenow.^{13,16} For construction of pSW-Apr and pSW-Tc, PCR
132 fragments amplified from pFLAG-attP (Addgene, #110095) with primers Apr fw/Apr rv and
133 from pSEVA524 with primers tetA fw/tetA rv,²⁵ respectively, using Q5 High-Fidelity Master
134 Mix (New England Biolabs) were cloned into pSW-I digested with ScaI.¹⁶

135 For in-frame deletion of *craA* (ABUW_0337) and *cmlA5* (ABUW_4059) pEMGT-*craA* and
136 pEMGT-*cmlA5* were constructed. For pEMGT-*craA*, 1 kb upstream and downstream
137 homologous regions were amplified from purified AB5075 genomic DNA with primers *craA*
138 up fw/*craA* up rv and *craA* down fw/*craA* down rv, respectively, and assembled together by
139 joining PCR. The same procedure was followed for assembly of the *cmlA5* deletion construct
140 using primer pairs *cmlA5* up fw/*cmlA5* up rv and *cmlA5* down fw/*cmlA5* down rv. Both
141 constructs were cloned into pEMGT digested with SmaI.

142 All plasmid derivatives were checked by colony PCR using DreamTaq Green PCR Master
143 Mix (ThermoFisher), restriction patterns and eventually by Sanger sequencing.

144

145 Triparental mating

146 For transfer of plasmid DNA into *A. baumannii* AB5075 and derivative strains, a standard
147 triparental mating protocol was followed, using pRK2013 (in a DH5 α host) as helper
148 plasmid and a DH5 α or a DH5 α *λpir* donor bearing the plasmid of interest.²⁶ For each
149 mating, 500 μ l of overnight cultures of the respective receptor, helper and donor strains were
150 mixed. Cells were pelleted by centrifugation and washed 2 times with fresh LB medium. The
151 final cell pellet was resuspended in 40 μ l of LB, spotted on a plain LB agar plate and left to
152 air-dry. After that, the biomass patch was incubated at 37 °C for 4 h. The biomass was then
153 resuspended in 1 ml of LB and serial dilutions were spread on the respective selective media
154 and on plain LB plates to assess viability and incubated at 37 °C overnight. Selection and
155 marker exchange were checked by multiple streaking on different selective LB plates

156 supplemented with ampicillin (to select AB5075 against *E. coli* strains) and the suitable
157 selective agent according to the resistance marker transferred plasmid. When necessary, DNA
158 deletions in the receptor strain were assessed by colony PCR and eventual Sanger sequencing
159 from PCR-amplified genomic DNA. Conjugation frequency was calculated as the number of
160 transconjugant colonies divided by the number of viable cells.

161

162 Antibiotic disc diffusion assay

163 Antibiotic sensitivity assays were performed in cation-adjusted (CaCl₂ 10 mM, MgCl₂ 5 mM)
164 Mueller-Hinton (pH 7.4) medium (CAMH, Sigma-Aldrich). Overnight cultures of *A.*
165 *baumannii* AB5075 or the respective mutant derivatives were diluted to 0.5 McFarland units
166 in CAMH broth and spread with a cotton swab on CAMH agar plates. When plates were dry,
167 chloramphenicol, amikacin or tobramycin discs (Oxoid) were placed in the middle of the
168 CAMH agar plate. Plates were incubated at 37 °C for 24 h before measuring the diameter of
169 the inhibition zone. Results are shown as averages of 3 biological replicates.

170

171 Minimum inhibitory concentration determination

172 Saturated overnight cultures were diluted in PBS (phosphate-buffered saline) to get an OD₆₀₀
173 0.2. The bacterial solutions were centrifuged at 6,000 rpm for 5 minutes and they were then
174 washed 3 times in PBS. Biomass was then resuspended in 1.2 ml of CAMH broth. The
175 dilution range of the antibiotic was prepared from a 50 mg/ml stock solution in CAMH broth.
176 The starting concentration of antibiotic in the range of dilution was 2500 µg/ml and was then
177 diluted 2-fold over 9 additional serial dilutions in CAMH broth.

178

179 In order of highest to lowest dilution, 100 µl of the antibiotic solution was added to each well
180 on a 96-well plate. Next, 100 µl of the cell suspension were added to each well. As control,
181 100 µl of sterile CAMH broth plus 100 µl of the bacterial solution and 200 µl of sterile
182 CAMHB were tested. The 96-well plate was then incubated at 37 °C, 200 rpm. Final OD₆₀₀
183 was measured after 16 h using a Clariostar Plus microplate reader (BMG LabTech). MICs
184 were assessed by visual examination, defining it as the lowest antibiotic concentration that
185 led to absence of visible bacteria growth.

186

187 **Results and discussion**

188 Rationale of the strategy

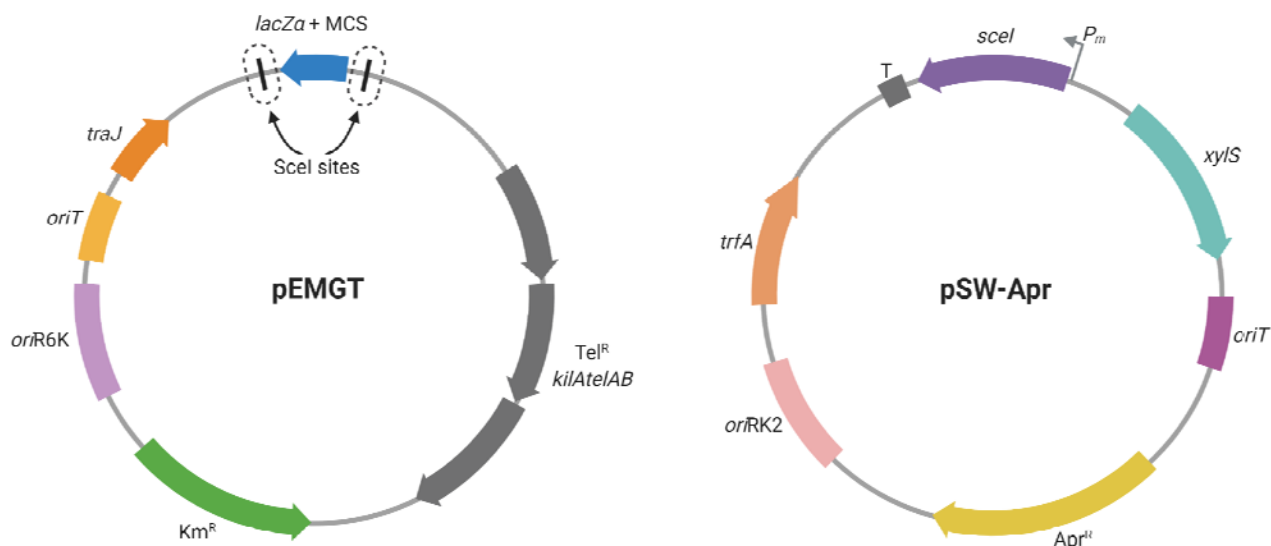
189 To adapt an efficient genome editing system for MDR *A. baumannii* AB5075, we built our
190 strategy on that by E. Martínez-García and V. de Lorenzo for *P. putida*,¹⁶ further optimised to
191 an accelerated version at the Nickel laboratory.^{16,21} To perform this strategy, plasmid pEMG
192 and pSW-I need to be used.¹⁶ pEMG is a cloning suicide vector bearing two target sites for
193 the endonuclease *SceI* flanking its polylinker. Once the homologous regions flanking the
194 desired modification are cloned into pEMG, the resulting plasmid is transferred to the target
195 strain and the integration in the genome is selected. Subsequently, the broad-host range pSW-
196 I plasmid, the *SceI* coding gene under an inducible *XylS*-dependent promoter, is introduced
197 in the co-integrate strain. Inducing the expression of *sceI* would trigger the double-strand
198 break in the genome that would eventually be repaired by homologous recombination,
199 generating the reversion to the parental strain genotype or the desired mutation. Apart from
200 improvements to make the screening more efficient, Wirth *et al.* introduced on-plate
201 induction of *sceI* expression,²¹ reducing the second recombination to one plasmid transfer and
202 selection step.

203 In the case of *A. baumannii* AB5075, one of the disadvantages for its genetic manipulation is
204 its resistance to most selectable markers, including those in pEMG and pSW-I. Hence, we
205 tackled the construction of a pEMG derivative bearing a tellurite resistance cassette as well as
206 its original kanamycin resistance gene. As a result, we obtained plasmid pEMG-TelR,
207 abbreviated pEMGT (Figure 1). For the second part of the strategy, we produced two variants
208 of the pSW-I plasmid, each bearing either an apramycin resistance marker or a tetracycline
209 resistance gene, namely pSW-Apr (Figure 1) and pSW-Tc, respectively. These plasmids
210 would serve as a platform for *A. baumannii* genome editing. To validate the method and
211 demonstrate its versatility, we attempted the construction of scar-free mutants in the
212 chromosome-encoded gene *craA* and the plasmid-borne gene *cmlA5*. Whereas *craA*
213 (identified in AB5075 by sequence similarity to the *craA* orthologue characterised in *A.*
214 *baumannii* ATCC 17978) is an efflux pump previously thought to be specific to
215 chloramphenicol,^{27,28} but recently shown to have a broader substrate range,²⁹ *cmlA5* is a
216 putative chloramphenicol efflux pump inferred from homology and encoded within an
217 aminoglycoside resistance island.²²

218

219

220



221

222 **Figure 1. Schematic representation of plasmids pEMGT and pSW-Apr.** All relevant
223 features borne in each plasmid are presented and named. Scel target sites in pEMGT are
224 circled in dotted lines. Adapted from “Custom Plasmid Maps 2”, by BioRender.com (2022).
225 Retrieved from <https://app.biorender.com/biorender-templates>

226

227

228 Deletion of *craA*

229 For the first trial of this genome editing method, we attempted the construction of an in-frame
230 deletion mutant in *craA* (ABUW_0337). A visual outline of the strategy can be followed in
231 Figure 2. Once the pEMGT derivative bearing the flanking homologous regions of *craA* was
232 constructed (pEMGT-*craA*), it was conjugated into the AB5075 parental strain and
233 transconjugants bearing the plasmid inserted by recombination were selected in the presence
234 of tellurite. Five candidates were confirmed to carry the plasmid integrated into the
235 chromosome by PCR (Supplementary Figure S1), and transconjugants appeared with
236 frequency of 10⁻⁸.

237 Among the candidates, three colonies were selected for performing the second recombination
238 event. To check the effectiveness of both pSW-Apr and pSW-Tc for forcing the second
239 recombination event, both of them were transferred by mating in biological triplicates to the
240 AB5075-pEMGT-*craA* parental strain and transconjugants were selected in the presence of
241 either antibiotic. We attempted the on-plate *scel* induction by adding the inducer 3-
242 methylbenzoate (3MB) to the selective plates. However, the presence of this compound
243 affected *A. baumannii* growth (Supplementary Figure S2). Nevertheless, this strategy has

244 been applied before without addition of the inducer,³⁰⁻³² which also resulted successful for *A.*
245 *baumannii*. In the case of pSW-Apr recipients, clear individual colonies grew with a
246 frequency around 10^{-4} . However, although pSW-Tc recipients grew with a similar frequency,
247 colonies appeared with a viscous, squashed phenotype (which we had previously observed
248 when selecting tetracycline resistance) that made selection difficult (Supplementary Figure
249 S3).

250 To assess the second recombination, we screened for the loss of tellurite resistance. This
251 screening resulted in 98.0 ± 1.7 % of clones that achieved a second recombination triggered
252 by presence of pSW-Apr (Figure 2) and 72.3 ± 3.2 % of clones by pSW-Tc.

253 To select a double recombinant carrying the in-frame deletion of *craA* instead of a reversion
254 to wild type genotype, 10 random candidates among all the pSW-Apr transconjugants were
255 streaked to obtain individual colonies and analysed by PCR. In this case, the screening
256 resulted in 100% deletion frequency according to the size of the PCR product.

257 As a final step in the protocol, the resulting mutant strain had to be cured from pSW-Apr. For
258 this, one mutant clone was inoculated in LB broth in the absence of apramycin and two
259 passages were given after reaching saturation. After this, individual colonies were isolated
260 and screened for apramycin sensitive clones. Chromosomal deletion was checked by
261 sequencing (Supplementary Figure S4, Supplementary File S1). To facilitate use of this
262 strategy, a detailed step-by-step laboratory protocol in 7-9 days is shown as Supplementary
263 Text S1.

264

265

266

267

268

269

270

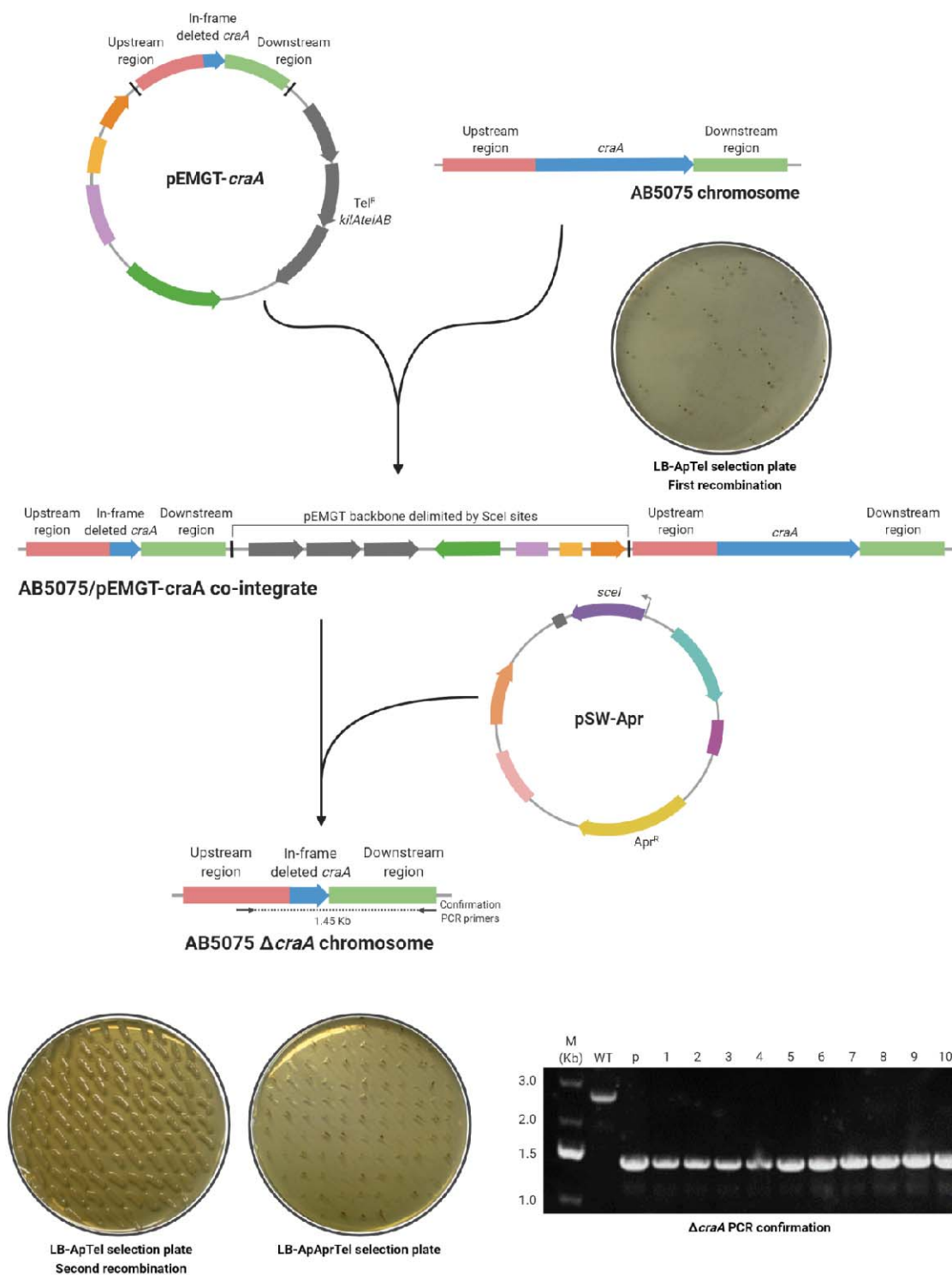
271

272

273

274

275



276 **Figure 2. Schematic outline of the genome editing strategy adapted for *A. baumannii***
 277 **AB5075 applied to the deletion of *craA*.** Plasmid features are represented as in Fig. 1. When
 278 indicated, LB agar plates were supplemented with ampicillin 100 mg/L (Ap), apramycin 200
 279 mg/L (Apr) and/or tellurite 30 mg/L (Tel). For confirmation of *craA* deletion, colony PCR
 280 was performed using primers *craA* fw seq and *craA* down rv. As controls, wild type AB5075
 281 (WT) and pEMGT-*craA* (p) were used. M: DNA molecular weight marker, with band sizes
 282 indicated in kilobases (Kb). Created with BioRender.com.

283 Deletion of *cmlA5* and removal of p1AB5075

284 In order to know if this mutagenesis system would be suitable for native plasmid editing
285 within *A. baumannii*, we challenged it by attempting the deletion of *cmlA5* (*ABUW_4059*).
286 This gene encodes a putative chloramphenicol efflux pump and is located within the so-called
287 resistance island 2 (RI2), borne in the p1AB5075 plasmid.^{22,33,34}
288 For the deletion, we performed a similar strategy as for the mutation of *craA*. Once the
289 respective flanking homologous regions were cloned into pEMGT (pEMGT-*cmlA5*), the
290 plasmid was transferred to AB5075 and its integration was selected for. For the second
291 recombination, we leaned toward using pSW-Apr, given its better performance compared to
292 pSW-Tc. After screening for a second recombination event, we checked 20 candidates by
293 PCR. In this particular case, we found that, whereas 35% of the clones had suffered a second
294 recombination (they gave a PCR of either wild type or mutant size), the remaining 65% did
295 not yield any amplification product. This would indicate that either a rearrangement in the
296 plasmid had occurred, removing the region that served as PCR template, or that the whole
297 plasmid had been removed. A possible explanation would be a scission of RI2 by
298 homologous recombination between the two miniature inverted-repeat transposable element
299 (MITE)-like sequences that flank this island, explaining the loss of the *cmlA5* region while
300 keeping the rest of p1AB5075.^{22,35} To address this, the same 20 candidates were analysed by
301 PCR with two primer pairs that had been used previously to check the presence of
302 p1AB5075.³⁶ This resulted in 20% of them not yielding a PCR product with any primer pair,
303 indicating the loss of the plasmid. One example of each template-primer pair combination is
304 shown in Figure 3.

305 Curing native plasmids, usually of unknown function, often involves tedious counterselection
306 screenings.³⁷⁻³⁹ Else, spontaneous plasmid-cured strains can be found serendipitously.^{36,40}
307 Given the high frequency of *A. baumannii* strains bearing multiple native plasmids and the
308 difficulties entailed by mutating and manipulating them, this methodology shows a
309 remarkable potential for their study.

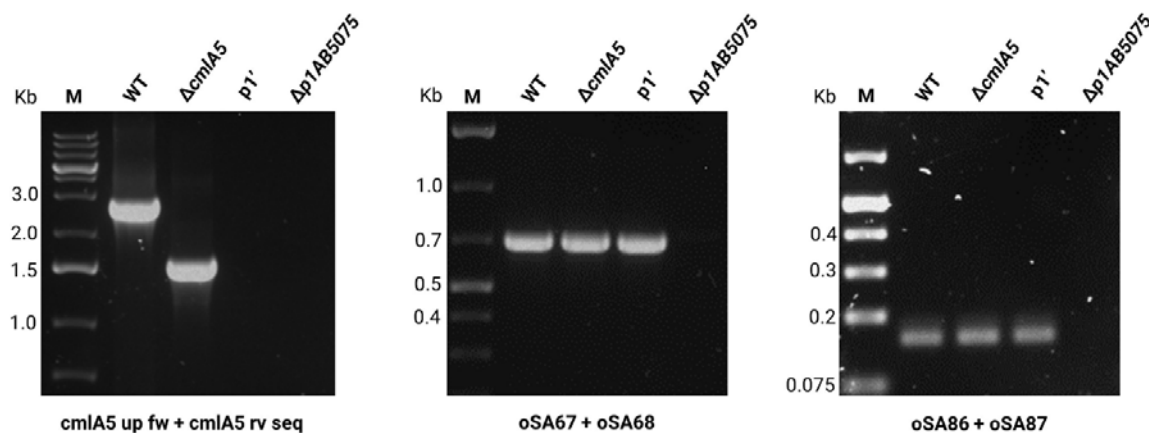
310

311

312

313

314



315 **Figure 3. PCR analysis to confirm the $\Delta cmlA5$ deletion and assess the presence of**
316 **p1AB5075.** Genomic DNA extracted from the respective strain was used as template. For
317 confirming the deletion, primer pair *cmlA5* up fw/*cmlA5* rv seq was used, giving bands of
318 2.79 Kb for the wild type (WT) and 1.55 Kb for the $\Delta cmlA5$ deletion mutant. The presence or
319 absence of p1AB5075 was assessed with primer pairs oSA67/oSA68 and oSA86/oSA87,
320 which would give PCR products of 0.7 Kb and 0.16 Kb, respectively (Anderson 2020). In the
321 case of the p1AB5075-cured strain, no amplification was observed for any of the primer
322 pairs. A plasmid rearrangement in p1AB5075 (p1') is suggested by the absence of PCR
323 product using the primers to detect *cmlA5* and compared to the amplification with primers to
324 confirm presence of p1AB5075. M: DNA molecular weight marker, with band sizes indicated
325 in Kb.

326

327

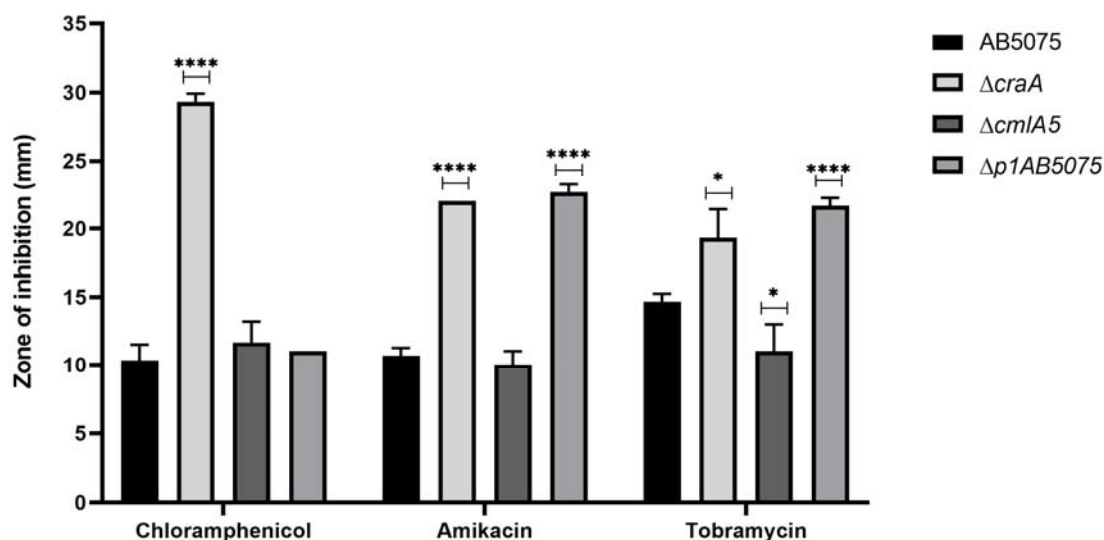
328

329 Phenotypic characterisation of the *craA* and *cmlA5* mutants

330 To assess the efficiency of this mutagenesis method, we chose to delete genes encoding for
331 antibiotic resistance, whose phenotype can be measured easily. Whereas there are reports
332 about the function of CraA,^{28,29} the RI2-encoded CmlA5 has only been annotated as a
333 chloramphenicol efflux pump based on homology.^{22,33,34} The phenotypic characterisation and
334 comparison of both mutants would help us elucidate the contribution of CmlA5 to antibiotic
335 resistance in AB5075.

336 For their characterisation, we assessed chloramphenicol resistance by disc diffusion assays
337 (DDA) and minimum inhibitory concentration (MIC) measurements comparing both deletion
338 mutants, as well as the p1AB5075-cured strain, to the wild type (Figure 4, Table 1,
339 Supplementary Figure S5). Whereas the DDAs showed that the $\Delta craA$ mutant was the only
340 one with an increased sensitivity to chloramphenicol (3.125 mg/L compared to 200 mg/L for
341 AB5075), the MIC assays revealed a mild increase in sensitivity for the $\Delta cmlA5$ mutant, that
342 kept increasing for the p1AB5075-cured strain (100 mg/L and 50 mg/L, respectively). This
343 indicates a minor role of *cmlA5* in chloramphenicol resistance in AB5075 and suggests there
344 are additional chloramphenicol resistance determinants encoded in p1AB5075.

345 Since *cmlA5* is located within RI2, likely forming an operon with genes related to
346 aminoglycoside resistance (*aadA1*, *strA*, *strB*), we wondered whether it could play a role in
347 resistance to this class of antibiotics.^{22,36} To address this, we performed DDAs and MIC
348 assays for the aminoglycosides amikacin and tobramycin for the two mutants and the
349 p1AB5075-cured strain compared to AB5075 (Figure 4, Table 1, Supplementary Figure S5).
350 Interestingly, whereas both DDAs and MICs showed that *cmlA5* is unrelated to
351 aminoglycoside resistance (same MICs for $\Delta cmlA5$ and AB5075), they showed that CraA
352 confers resistance to amikacin and tobramycin, with MICs dropping more than 130-fold. As
353 expected, the loss of p1AB5075 led to a substantial reduction in aminoglycoside resistance,
354 particularly to tobramycin. It was also worth mentioning a slight increase in resistance to
355 tobramycin for the $\Delta cmlA5$ mutant. Since *cmlA5* is likely the first of an operon formed with
356 other three genes related to antibiotic resistance, it would be possible that its deletion minorly
357 altered the expression of the following genes, thus leading to this mild increase.
358 Although CraA was previously thought to confer resistance specifically to chloramphenicol,²⁸
359 it was recently shown to have a broader substrate range.²⁹ Consequently, it was postulated to
360 be closer in function to the multidrug efflux pump MdfA, although differing in the substrate
361 recognition mechanism.²⁹ Here, we expand the CraA substrate spectrum even further by
362 demonstrating its role in aminoglycoside resistance. Altogether, this indicates that CraA
363 might play a major role in *A. baumannii* multidrug resistance.
364



365 **Figure 4. Antibiotic disc diffusion assay for the Δ *craA* and Δ *cmlA5* mutants and**
 366 **$p1AB5075$ -cured strain compared to the wild type AB5075.** Assays were performed in
 367 CAMH agar assessing sensitivity to imipenem (10 μ g) as control (no increase in sensitivity
 368 was expected for imipenem in these strains compared to AB5075), chloramphenicol (50 μ g),
 369 amikacin (30 μ g) and tobramycin (10 μ g). The average zone of inhibition in millimetres
 370 (mm) measured from 3 biological replicates \pm S.D. is shown. Statistical significance was
 371 assessed from P-values obtained from a t-test (* = $P \leq 0.05$, ** = $P \leq 0.01$, **** = $P \leq 0.0001$).
 372

	AB5075	Δ <i>craA</i>	Δ <i>cmlA5</i>	Δ <i>p1AB5075</i>
Chloramphenicol	200 mg/L	3.125 mg/L	100 mg/L	50 mg/L
Amikacin	200 mg/L	1.5625 mg/L	200 mg/L	3.125 mg/L
Tobramycin	25 mg/L	1.5625 mg/L	25 mg/L	< 0.781 mg/L

373

374 **Table 1. Minimum inhibitory concentration (MIC) for the Δ *craA* and Δ *cmlA5* mutants**
 375 **and the $p1AB5075$ -cured strain (Δ *p1AB5075*) compared to the wild type AB5075.** MICs
 376 were assessed in CAMH broth. Antibiotics were diluted by 2-fold, ranging from 400 mg/L to
 377 0.781 mg/L, except for tobramycin when used against the Δ *craA* mutant, which ranged from
 378 100 mg/L to 0.195 mg/L. The MIC was assessed as the first concentration that showed no
 379 visual growth. Three biological replicates were conducted.

380

381

382 **References**

- 383 1. Harding CM, Hennon SW, Feldman MF. Uncovering the mechanisms of
384 *Acinetobacter baumannii* virulence. Nat Rev Microbiol 2018; 16(2) : 91-102.
- 385 2. McCarthy RR, Larrouy-Maumus GJ, Meiqi Tan MGC et al. Antibiotic Resistance
386 Mechanisms and Their Transmission in *Acinetobacter baumannii*. In: Kishore U, ed.
387 Microbial Pathogenesis. Advances in Experimental Medicine and Biology.
388 Switzerland: Springer Cham, 2021; 1313 : 135-153.
- 389 3. Jacobs AC, Thompson MG, Black CC et al. AB5075, a Highly Virulent Isolate of
390 *Acinetobacter baumannii*, as a Model Strain for the Evaluation of Pathogenesis and
391 Antimicrobial Treatments. mBio, 2014; 5(3) : e01076-14.
- 392 4. Kröger C, Kary SC, Schauer K et al. Genetic Regulation of Virulence and Antibiotic
393 Resistance in *Acinetobacter baumannii*. Genes (Basel), 2016; 8(1) : 12.
- 394 5. Karlowsky JA, Hoban DJ, Hackel MA et al. Antimicrobial susceptibility of Gram-
395 negative ESKAPE pathogens isolated from hospitalized patients with intra-abdominal
396 and urinary tract infections in Asia-Pacific countries: SMART 2013-2015. J Med
397 Microbiol, 2017; 66(1) : 61-69.
- 398 6. Pendleton JN, Gorman SP, Gilmore BF. Clinical relevance of the ESKAPE
399 pathogens. Expert Rev Anti Infect Ther, 2013; 11(3) : 297-308.
- 400 7. Tacconelli E, Carrara E, Savoldi A et al. WHO Pathogens Priority List Working
401 Group. Discovery, research, and development of new antibiotics: the WHO priority
402 list of antibiotic-resistant bacteria and tuberculosis. Lancet Infect Dis, 2018; 18(3) :
403 318-327.
- 404 8. Fournier PE, Richet H. The epidemiology and control of *Acinetobacter baumannii* in
405 health care facilities. Clin Infect Dis, 2006 42(5) : 692-9.
- 406 9. Pagano M, Martins AF, Barth AL. Mobile genetic elements related to carbapenem
407 resistance in *Acinetobacter baumannii*. Braz J Microbiol, 2016; 47(4) : 785-792.
- 408 10. Almasaudi SB. *Acinetobacter* spp. as nosocomial pathogens: Epidemiology and
409 resistance features. Saudi J Biol Sci, 2018; 25(3) : 586-596.
- 410 11. Aranda J, Poza M, Pardo BG et al. A rapid and simple method for constructing stable
411 mutants of *Acinetobacter baumannii*. BMC Microbiol, 2010; 10 : 279.
- 412 12. Tucker AT, Nowicki EM, Boll JM et al. Defining gene-phenotype relationships in
413 *Acinetobacter baumannii* through one-step chromosomal gene inactivation. mBio,
414 2014; 5(4) : e01313-14.

- 415 **13.** Amin IM, Richmond GE, Sen P et al. A method for generating marker-less gene
416 deletions in multidrug-resistant *Acinetobacter baumannii*. BMC Microbiol, 2013; 13 :
417 158.
- 418 **14.** Bai J, Dai Y, Farinha A et al. Essential Gene Analysis in *Acinetobacter baumannii* by
419 High-Density Transposon Mutagenesis and CRISPR Interference. J Bacteriol, 2021;
420 203(12) : e0056520.
- 421 **15.** Hoang TT, Karkhoff-Schweizer RR, Kutchma AJ et al. A broad-host-range Flp-FRT
422 recombination system for site-specific excision of chromosomally-located DNA
423 sequences: application for isolation of unmarked *Pseudomonas aeruginosa* mutants.
424 Gene, 1998; 212(1) : 77-86.
- 425 **16.** Martínez-García E, de Lorenzo V. Engineering multiple genomic deletions in Gram-
426 negative bacteria: analysis of the multi-resistant antibiotic profile of *Pseudomonas*
427 *putida* KT2440. Environ Microbiol, 2011; 13(10) : 2702-16.
- 428 **17.** Pósfai G, Kolisnychenko V, Bereczki Z et al. Markerless gene replacement in
429 *Escherichia coli* stimulated by a double-strand break in the chromosome. Nucleic
430 Acids Res, 1999; 27(22) : 4409-15.
- 431 **18.** Wong SM, Mekalanos JJ. Genetic footprinting with mariner-based transposition in
432 *Pseudomonas aeruginosa*. Proc Natl Acad Sci U S A, 2000; 97(18) : 10191-6.
- 433 **19.** Flanagan RS, Linn T, Valvano MA. A system for the construction of targeted
434 unmarked gene deletions in the genus Burkholderia. Environ Microbiol, 2008; 10(6) :
435 1652-60.
- 436 **20.** López CM, Rholl DA, Trunck LA et al. Versatile dual-technology system for
437 markerless allele replacement in *Burkholderia pseudomallei*. Appl Environ Microbiol,
438 2009; 75(20) : 6496-503.
- 439 **21.** Wirth NT, Kozaeva E, Nickel PI. Accelerated genome engineering of *Pseudomonas*
440 *putida* by I-SceI-mediated recombination and CRISPR-Cas9 counterselection. Microb
441 Biotechnol, 2020; 13(1) : 233-249.
- 442 **22.** Gallagher LA, Ramage E, Weiss EJ et al. Resources for Genetic and Genomic
443 Analysis of Emerging Pathogen *Acinetobacter baumannii*. J Bacteriol, 2015; 197(12)
444 : 2027-35.
- 445 **23.** Chin CY, Tipton KA, Farokhyfar M et al. A high-frequency phenotypic switch links
446 bacterial virulence and environmental survival in *Acinetobacter baumannii*. Nat
447 Microbiol, 2018; 3(5) : 563-569.

- 448 **24.** Hanahan D. Studies on transformation of *Escherichia coli* with plasmids. J Mol Biol,
449 1983; 166(4) : 557-80.
- 450 **25.** Silva-Rocha R, Martínez-García E, Calles B et al. The Standard European Vector
451 Architecture (SEVA): a coherent platform for the analysis and deployment of
452 complex prokaryotic phenotypes. Nucleic Acids Res, 2013; 41(Database issue) :
453 D666-75.
- 454 **26.** Figurski DH, Helinski DR. Replication of an origin-containing derivative of plasmid
455 RK2 dependent on a plasmid function provided in trans. Proc. Natl. Acad. Sci. U.S.A.,
456 1979; 76 : 1648-1652.
- 457 **27.** Kröger C, MacKenzie KD, Alshabib EY et al. The primary transcriptome, small
458 RNAs and regulation of antimicrobial resistance in *Acinetobacter baumannii* ATCC
459 17978. Nucleic Acids Res, 2018; 46(18) : 9684-9698.
- 460 **28.** Roca I, Marti S, Espinal P et al. CraA, a major facilitator superfamily efflux pump
461 associated with chloramphenicol resistance in *Acinetobacter baumannii*. Antimicrob
462 Agents Chemother, 2009; 53(9) : 4013-4.
- 463 **29.** Foong WE, Tam HK, Cames JJ et al. The chloramphenicol/H⁺ antiporter CraA of
464 *Acinetobacter baumannii* AYE reveals a broad substrate specificity. J Antimicrob
465 Chemother, 2019; 74(5) : 1192-1201.
- 466 **30.** González-Flores YE, de Dios R, Reyes-Ramírez F et al. The response of *Sphingopyxis*
467 *granuli* strain TFA to the hostile anoxic condition. Sci Rep, 2019; 9(1) : 6297.
- 468 **31.** de Dios R, Santero E, Reyes-Ramírez F. The functional differences between
469 paralogous regulators define the control of the general stress response in *Sphingopyxis*
470 *granuli* □ □ TFA. Environ Microbiol, 2022; In Press. doi: 10.1111/1462-2920.15907.
- 471 **32.** de Dios R, Rivas-Marin E, Santero E, Reyes-Ramírez F. Two paralogous EcfG σ
472 factors hierarchically orchestrate the activation of the General Stress Response in
473 *Sphingopyxis granuli* TFA. Sci Rep, 2020; 10(1) : 5177.
- 474 **33.** Vila J, Martí S, Sánchez-Céspedes J. Porins, efflux pumps and multidrug resistance in
475 *Acinetobacter baumannii*. J Antimicrob Chemother, 2007; 59(6) : 1210-5.
- 476 **34.** Fournier PE, Vallenet D, Barbe V et al. Comparative genomics of multidrug
477 resistance in *Acinetobacter baumannii*. PLoS Genet, 2006; 2(1) : e7.
- 478 **35.** Gillings MR, Labbate M, Sajjad A et al. Mobilization of a Tn402-like class 1 integron
479 with a novel cassette array via flanking miniature inverted-repeat transposable
480 element-like structures. Appl Environ Microbiol, 2009; 75(18) : 6002-4.

- 481 **36.** Anderson SE, Chin CY, Weiss DS et al. Copy Number of an Integron-Encoded
482 Antibiotic Resistance Locus Regulates a Virulence and Opacity Switch in
483 *Acinetobacter baumannii* AB5075. *mBio*, 2020; 11(5) : e02338-20.
- 484 **37.** Ohtani N, Tomita M, Itaya M. Curing the Megaplasmid pTT27 from *Thermus*
485 *thermophilus* HB27 and Maintaining Exogenous Plasmids in the Plasmid-Free Strain.
486 *Appl Environ Microbiol*, 2015; 82(5) : 1537-48.
- 487 **38.** Oresnik IJ, Liu SL, Yost CK, Hynes MF. Megaplasmid pRme2011a of *Sinorhizobium*
488 *meliloti* is not required for viability. *J Bacteriol*, 2000; 182(12) : 3582-3586.
- 489 **39.** Romanchuk A, Jones CD, Karkare K et al. Bigger is not always better: transmission
490 and fitness burden of ~1MB *Pseudomonas syringae* megaplasmid pMPPla107.
491 *Plasmid*, 2014; 73 : 16-25.
- 492 **40.** Di Venanzio G, Flores-Mireles AL, Calix JJ et al. Urinary tract colonization is
493 enhanced by a plasmid that regulates uropathogenic *Acinetobacter baumannii*
494 chromosomal genes. *Nat Commun*, 2019; 10(1) : 2763.

495 **Acknowledgements**

496 The authors would like to thank Dr Esteban Martínez-García and Prof Víctor de Lorenzo
497 (Centro Nacional de Biotecnología, Madrid, Spain) for providing pEMG, pSW-I and
498 pSEVA524 as a kind gift. RRMC is supported by the British Society for Antimicrobial
499 Chemotherapy BSAC-2018-0095. RRMC and RD are supported by a BBSRC New
500 Investigator Award BB/V007823/1. RRMC is supported by the Academy of Medical
501 Sciences/the Wellcome Trust/ the Government Department of Business, Energy and
502 Industrial Strategy/the British Heart Foundation/Diabetes UK Springboard Award
503 [SBF006\1040].

504

505 **Author contribution**

506 RD and RRMC designed the strategy and the experimental work. RD and KG performed the
507 experiments and analysed the results. RD, KG and RRMC wrote and reviewed the
508 manuscript.

509

510 **Data Availability**

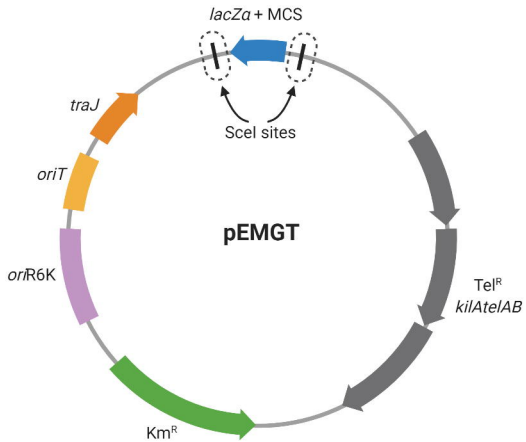
511 All plasmids available through request to the corresponding author.

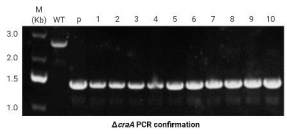
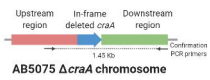
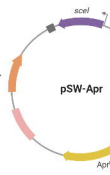
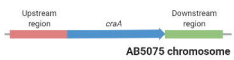
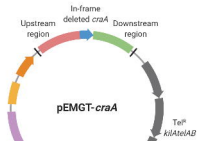
512

513 **Transparency declarations**

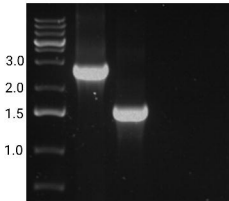
514 The authors declare no competing interests.

515



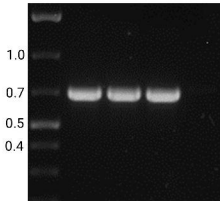


Kb M WT Δ *cmlA5* *p1'* Δ *p1AB5075*



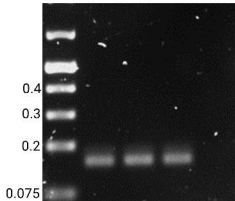
cmlA5 up fw + *cmlA5* rv seq

Kb M WT Δ *cmlA5* *p1'* Δ *p1AB5075*



oSA67 + *oSA68*

Kb M WT Δ *cmlA5* *p1'* Δ *p1AB5075*



oSA86 + *oSA87*

